

Double ionization of helium by fast bare ion collisions

M S Pindzola¹, F Robicheaux¹ and J Colgan²

¹ Department of Physics, Auburn University, Auburn, AL 36849

² Theoretical Division, Los Alamos National Laboratory, Los Alamos, NM 87545, USA

Received 10 January 2007, in final form 13 February 2007

Published 30 April 2007

Online at stacks.iop.org/JPhysB/40/1695

Abstract

A time-dependent close-coupling method is developed to treat the double ionization of helium by fast bare ion collisions. At high incident energies, charge transfer to the projectile is quite small, so that the two-electron wavefunction remains centred on the target, subject to a time-dependent projectile interaction. A multipole expansion of the projectile–atom interaction includes monopole, dipole, quadrupole and octopole terms. Time-dependent close-coupling calculations are carried out for $\alpha + \text{He}$ collisions at incident energies greater or equal to 1.0 MeV amu⁻¹. Over 100 coupled channels are needed to obtain total double ionization cross sections that are in good agreement with recent non-perturbative basis-set coupled channels calculations and absolute experimental measurements.

1. Introduction

The simultaneous ejection of both electrons from the helium atom is one of nature's clearest examples of quantal three-body breakup. For small angles between slow moving ejected electrons, the highly correlated motion becomes difficult for all perturbative approaches. In the last few years, a number of non-perturbative quantal methods have been applied to calculate double photoionization processes in helium. The single-photon double ionization of the ground state of helium has been calculated using the convergent close-coupling [1], time-dependent close-coupling [2], hyperspherical *R*-matrix [3], B-spline *R*-matrix [4] and exterior complex scaling [5] methods. The level of agreement between the various non-perturbative theories and experimental measurements using synchrotron light sources for total energy differential and angle differential cross sections has generally been excellent.

Recently, a non-perturbative quantal method, based on a coupled basis-set solution of the time-dependent Schrödinger equation, was applied to calculate the double ionization of helium in heavy-ion collisions [6, 7]. Where before perturbative methods [8, 9] predicted double ionization cross sections for $\alpha + \text{He}$ collisions between 0.9 and 2.0 times absolute experimental measurements [10, 11], the new non-perturbative results are within the experimental error bars.

In this paper, we develop a non-perturbative time-dependent close-coupling method to calculate double ionization processes in fast bare ion collisions with helium. At high incident

energies, charge transfer to the projectile is quite small, so that the two-electron wavefunction remains centred on the target, subject to a time-dependent projectile interaction. Thus, a partial wave expansion for the two-electron wavefunction in a target centred spherical polar coordinate system reduces the time-dependent Schrödinger equation to a coupled set of partial differential equations in a manner similar to that found before [12, 13] for photoionization processes. In general, however, the number of contributing terms in the multipole expansion for the electron–bare ion interaction is greater than the number needed for the electron–photon interaction. Besides a strong dipole interaction, we find that monopole, quadrupole and octopole terms must be included in the electron–bare ion interaction. The need for consideration of polarization in the photoionization processes is replaced by the need for consideration of impact parameters in the bare ion ionization processes, while consideration of intensity and pulse length in the photoionization processes is replaced by consideration of projectile charge and velocity in the bare ion ionization processes. To compare with previous non-perturbative calculations [7] and absolute experimental measurements [10, 11], we apply the time-dependent close-coupling method to calculate double ionization cross sections for $\alpha + \text{He}$ collisions at incident energies greater or equal to 1.0 MeV amu⁻¹. At these energies, charge transfer processes are too small to be even measured [11]; therefore, a time-dependent close-coupling method that ignores charge transfer processes should yield accurate double ionization cross section results.

The rest of the paper is organized as follows. In section 2, we develop a time-dependent close-coupling method for ionization processes in fast bare ion collisions with helium. In section 3, we apply the time-dependent close coupling to calculate ionization processes in $\alpha + \text{He}$ collisions and compare with experimental measurements. In section 4, we conclude with a brief summary and outlook for future work. Unless otherwise stated, all quantities are given in atomic units.

2. Theory

The fully correlated wavefunction, $\Phi^{L_0 M_0}$, for the ground state of a two-electron target atom is obtained by relaxation of the time-dependent Schrödinger equation in imaginary time ($\tau = it$):

$$-\frac{\partial \Phi^{L_0 M_0}(\vec{r}_1, \vec{r}_2, \tau)}{\partial \tau} = H_{\text{target}} \Phi^{L_0 M_0}(\vec{r}_1, \vec{r}_2, \tau), \quad (1)$$

where the non-relativistic Hamiltonian is given by

$$H_{\text{target}} = \sum_{i=1}^2 \left(-\frac{1}{2} \nabla_i^2 - \frac{Z_t}{r_i} \right) + \frac{1}{|\vec{r}_1 - \vec{r}_2|} \quad (2)$$

and Z_t is the target atomic number.

The fully correlated wavefunction, Ψ^{LM} , for the ionization of a two-electron target atom by a fast, fully-stripped atomic ion is obtained by evolution of the time-dependent Schrödinger equation in real time:

$$i \frac{\partial \Psi^{LM}(\vec{r}_1, \vec{r}_2, t)}{\partial t} = H_{\text{system}} \Psi^{LM}(\vec{r}_1, \vec{r}_2, t), \quad (3)$$

where the non-relativistic Hamiltonian is given by

$$H_{\text{system}} = H_{\text{target}} - \frac{Z_p}{|\vec{r}_1 - \vec{R}(t)|} - \frac{Z_p}{|\vec{r}_2 - \vec{R}(t)|} \quad (4)$$

and Z_p is the projectile atomic number. For straight-line motion, the magnitude of the time-dependent projectile position is given by

$$R(t) = \sqrt{b^2 + (d_0 + vt)^2}, \quad (5)$$

where b is an impact parameter, d_0 is a starting distance ($d_0 < 0$), and v is the projectile speed.

If we expand $\Phi^{L_0 M_0}$ in coupled spherical harmonics and substitute into equation (1), the resulting close-coupled equations for the $\bar{P}_{l_1 l_2}^{L_0 M_0}(r_1, r_2, \tau)$ radial expansion functions are given by

$$-\frac{\partial \bar{P}_{l_1 l_2}^{L_0 M_0}(r_1, r_2, \tau)}{\partial \tau} = T_{l_1 l_2}(r_1, r_2) \bar{P}_{l_1 l_2}^{L_0 M_0}(r_1, r_2, \tau) + \sum_{l'_1, l'_2} V_{l_1 l_2, l'_1 l'_2}^{L_0}(r_1, r_2) \bar{P}_{l'_1 l'_2}^{L_0 M_0}(r_1, r_2, \tau), \quad (6)$$

where

$$T_{l_1 l_2}(r_1, r_2) = -\frac{1}{2} \frac{\partial^2}{\partial r_1^2} - \frac{1}{2} \frac{\partial^2}{\partial r_2^2} + \frac{l_1(l_1 + 1)}{2r_1^2} + \frac{l_2(l_2 + 1)}{2r_2^2} - \frac{Z_t}{r_1} - \frac{Z_t}{r_2} \quad (7)$$

and

$$V_{l_1 l_2, l'_1 l'_2}^L(r_1, r_2) = (-1)^{L+l_2+l'_2} \sqrt{(2l_1 + 1)(2l'_1 + 1)(2l_2 + 1)(2l'_2 + 1)} \\ \times \sum_{\lambda} \frac{(r_1, r_2)_{<}^{\lambda}}{(r_1, r_2)_{>}^{\lambda+1}} \begin{pmatrix} l_1 & \lambda & l'_1 \\ 0 & 0 & 0 \end{pmatrix} \begin{pmatrix} l_2 & \lambda & l'_2 \\ 0 & 0 & 0 \end{pmatrix} \left\{ \begin{matrix} L & l'_2 & l'_1 \\ \lambda & l_1 & l_2 \end{matrix} \right\}. \quad (8)$$

The initial value boundary condition for equation (6) is given by

$$\bar{P}_{l_1 l_2}^{L_0 M_0}(r_1, r_2, \tau = 0) = P_{1s}(r_1) P_{1s}(r_2), \quad (9)$$

where $P_{1s}(r)$ is a single particle bound radial orbital for the one-electron target ion with $L_0 = M_0 = 0$.

If we expand Ψ^{LM} in coupled spherical harmonics and substitute into equation (3), the resulting close-coupled equations for the $P_{l_1 l_2}^{LM}(r_1, r_2, t)$ radial expansion functions are given by

$$i \frac{\partial P_{l_1 l_2}^{LM}(r_1, r_2, t)}{\partial t} = T_{l_1 l_2}(r_1, r_2) P_{l_1 l_2}^{LM}(r_1, r_2, t) + \sum_{l'_1, l'_2} V_{l_1 l_2, l'_1 l'_2}^L(r_1, r_2) P_{l'_1 l'_2}^{LM}(r_1, r_2, t) \\ + \sum_{L', M'} \sum_{l'_1, l'_2} W_{l_1 l_2, l'_1 l'_2}^{LM, L'M'}(r_1, R(t)) P_{l'_1 l'_2}^{L'M'}(r_1, r_2, t) \\ + \sum_{L', M'} \sum_{l'_1, l'_2} W_{l_1 l_2, l'_1 l'_2}^{LM, L'M'}(r_2, R(t)) P_{l'_1 l'_2}^{L'M'}(r_1, r_2, t), \quad (10)$$

where

$$W_{l_1 l_2, l'_1 l'_2}^{LM, L'M'}(r_1, R(t)) = -Z_p \delta_{l_2, l'_2} (-1)^{l_2+L+L'-M} \sqrt{(2l_1 + 1)(2l'_1 + 1)(2L + 1)(2L' + 1)} \\ \times \sum_{\lambda} (-1)^{\lambda} \frac{(r_1, R(t))_{<}^{\lambda}}{(r_1, R(t))_{>}^{\lambda+1}} \begin{pmatrix} l_1 & \lambda & l'_1 \\ 0 & 0 & 0 \end{pmatrix} \\ \times \sum_q C_q^{\lambda*}(\theta, \phi) \begin{pmatrix} L & \lambda & L' \\ -M & q & M' \end{pmatrix} \left\{ \begin{matrix} l_1 & l_2 & L \\ L' & \lambda & l'_1 \end{matrix} \right\} \quad (11)$$

and

$$W_{l_1 l_2, l'_1 l'_2}^{LM, L'M'}(r_2, R(t)) = -Z_p \delta_{l_1, l'_1} (-1)^{l_1+l_2+l'_2-M} \sqrt{(2l_2 + 1)(2l'_2 + 1)(2L + 1)(2L' + 1)} \\ \times \sum_{\lambda} (-1)^{\lambda} \frac{(r_2, R(t))_{<}^{\lambda}}{(r_2, R(t))_{>}^{\lambda+1}} \begin{pmatrix} l_2 & \lambda & l'_2 \\ 0 & 0 & 0 \end{pmatrix} \\ \times \sum_q C_q^{\lambda*}(\theta, \phi) \begin{pmatrix} L & \lambda & L' \\ -M & q & M' \end{pmatrix} \left\{ \begin{matrix} l_1 & l_2 & L \\ \lambda & L' & l'_2 \end{matrix} \right\}. \quad (12)$$

The spherical tensor in equations (11)–(12) is defined by

$$C_q^\lambda(\theta, \phi) = \sqrt{\frac{4\pi}{2\lambda + 1}} Y_q^\lambda(\theta, \phi), \quad (13)$$

where $Y_q^\lambda(\theta, \phi)$ is a spherical harmonic. If the projectile follows a straight-line trajectory in the xz plane with $\vec{R}(t) = b\hat{i} + (d_0 + vt)\hat{k}$, then $\sin\theta = \frac{b}{R(t)}$, $\cos\theta = \frac{(d_0 + vt)}{R(t)}$, $\phi = 0$, and the spherical tensor is real. If the projectile follows a straight-line trajectory in the xy plane with $\vec{R}(t) = b\hat{i} + (d_0 + vt)\hat{j}$, then $\theta = \frac{\pi}{2}$, $\sin\phi = \frac{(d_0 + vt)}{R(t)}$, $\cos\phi = \frac{b}{R(t)}$, and the spherical tensor is complex. The initial value boundary condition for equation (10) is given by

$$P_{l_1 l_2}^{LM}(r_1, r_2, t = 0) = \delta_{L, L_0} \delta_{M, M_0} \bar{P}_{l_1 l_2}^{L_0 M_0}(r_1, r_2, \tau \rightarrow \infty). \quad (14)$$

We solve the time-dependent close-coupling equations, found in equations (6) and (10), using lattice techniques to obtain a discrete representation of the radial expansion functions, $\bar{P}_{l_1 l_2}^{L_0 M_0}(r_1, r_2, \tau)$ and $P_{l_1 l_2}^{LM}(r_1, r_2, t)$, and all operators on a two-dimensional grid. The grid is partitioned into small squares for distribution among the processors on a massively parallel computer, so-called domain decomposition.

For ionization probabilities, we begin by defining asymptotic radial expansion functions. For the $l_1 l_2 L_0 M_0$ channels,

$$P_{l_1 l_2}^{L_0 M_0}(r_1, r_2) = P_{l_1 l_2}^{L_0 M_0}(r_1, r_2, t \rightarrow \infty) - \mathcal{L} \bar{P}_{l_1 l_2}^{L_0 M_0}(r_1, r_2, \tau \rightarrow \infty), \quad (15)$$

and for all other $l_1 l_2 LM$ channels,

$$P_{l_1 l_2}^{LM}(r_1, r_2) = P_{l_1 l_2}^{LM}(r_1, r_2, t \rightarrow \infty), \quad (16)$$

where the overlap factor is given by

$$\mathcal{L} = \sum_{l_1, l_2} \int_0^\infty dr_1 \int_0^\infty dr_2 \bar{P}_{l_1 l_2}^{L_0 M_0}(r_1, r_2, \tau \rightarrow \infty) P_{l_1 l_2}^{L_0 M_0}(r_1, r_2, t \rightarrow \infty). \quad (17)$$

The total single ionization probability, for a given velocity and impact parameter, may be calculated in either of two ways. The expression involving only bound $P_{nl}(r)$ single particle orbitals is given by

$$\begin{aligned} \mathcal{P}_{\text{ion}}(v, b) = & \sum_{l_1, l_2, L, M} \sum_n \left(\int_0^\infty dr_2 \left| \int_0^\infty dr_1 P_{nl_1}(r_1) P_{l_1 l_2}^{LM}(r_1, r_2) \right|^2 \right. \\ & - \sum_{n'} \left| \int_0^\infty dr_1 \int_0^\infty dr_2 P_{nl_1}(r_1) P_{n'l_2}(r_2) P_{l_1 l_2}^{LM}(r_1, r_2) \right|^2 \\ & + \int_0^\infty dr_1 \left| \int_0^\infty dr_2 P_{nl_2}(r_2) P_{l_1 l_2}^{LM}(r_1, r_2) \right|^2 \\ & \left. - \sum_{n'} \left| \int_0^\infty dr_1 \int_0^\infty dr_2 P_{n'l_1}(r_1) P_{nl_2}(r_2) P_{l_1 l_2}^{LM}(r_1, r_2) \right|^2 \right). \quad (18) \end{aligned}$$

The expression involving both bound $P_{nl}(r)$ and continuum $P_{kl}(r)$ single particle states is given by

$$\begin{aligned} \mathcal{P}_{\text{ion}}(v, b) = & \sum_{l_1, l_2, L, M} \sum_n \int_0^\infty dk \left(\left| \int_0^\infty dr_1 \int_0^\infty dr_2 P_{nl_1}(r_1) P_{kl_2}(r_2) P_{l_1 l_2}^{LM}(r_1, r_2) \right|^2 \right. \\ & \left. + \left| \int_0^\infty dr_1 \int_0^\infty dr_2 P_{kl_1}(r_1) P_{nl_2}(r_2) P_{l_1 l_2}^{LM}(r_1, r_2) \right|^2 \right). \quad (19) \end{aligned}$$

Using only bound $P_{nl}(r)$ single particle orbitals, the total double ionization probability is given by

$$\mathcal{P}_{\text{dion}}(v, b) = \sum_{l_1, l_2, L, M} \int_0^\infty dr_1 \int_0^\infty dr_2 |P_{l_1 l_2}^{LM}(r_1, r_2)|^2 - \mathcal{P}_{\text{sion}}(v, b) - \sum_{l_1, l_2, L, M} \sum_n \sum_{n'} \left| \int_0^\infty dr_1 \int_0^\infty dr_2 P_{nl_1}(r_1) P_{n'l_2}(r_2) P_{l_1 l_2}^{LM}(r_1, r_2) \right|^2. \quad (20)$$

Using only continuum $P_{kl}(r)$ single particle orbitals, the total double ionization probability is given by

$$\mathcal{P}_{\text{dion}}(v, b) = \sum_{l_1, l_2, L, M} \int_0^\infty dk_1 \int_0^\infty dk_2 \left| \int_0^\infty dr_1 \int_0^\infty dr_2 P_{k_1 l_1}(r_1) P_{k_2 l_2}(r_2) P_{l_1 l_2}^{LM}(r_1, r_2) \right|^2. \quad (21)$$

The bound $P_{nl}(r)$ and continuum $P_{kl}(r)$ single particle orbitals found in equations (18)–(21) are calculated by direct diagonalization of the time-independent radial Schrödinger equation for the one-electron target ion. The one-dimensional grid for the diagonalization has the same mesh spacing and extent as that used for the two-electron system. Finally, for both single and double ionizations, the total cross section for a given velocity is given by

$$\sigma(v) = 2\pi \int_0^\infty \mathcal{P}(v, b) b db. \quad (22)$$

3. Results

The time-dependent close-coupling method was used to calculate the ground state of He using equation (6). We employed a 384×384 point radial lattice with a uniform mesh spacing of $\Delta r = 0.20$, and thus a box size of $R = 76.8$. For four coupled channels ($l_1 l_2 L_0 M_0 = \text{ss00, pp00, dd00, ff00}$), a fully converged ground state of He on the lattice yielded a total energy of -75.8 eV. The infinite lattice limit is -79.0 eV. A mesh spacing of $\Delta r = 0.20$ was used before to study the two-photon double ionization of He and H^- [12].

The time-dependent close-coupling method was then used to calculate ionization cross sections for $\alpha + \text{He}$ collisions using equation (10) at incident energies of 1.000, 1.280 and 1.585 MeV amu^{-1} . At these energies charge transfer processes are too small to be even measured [11]. For the 34 coupled channels found in table 1, and for $\lambda \leq 3$ multipole contributions in the W operators of equations (11) and (12), the single ionization cross sections are compared with basis-set coupled channels calculations [7] and absolute experimental measurements [10, 11] in figure 1. The 34 coupled channels include ($s \rightarrow p, s \rightarrow d, s \rightarrow f$) promotions from the dominant uncorrelated ss ground state. The time-dependent close-coupling results for single ionization are found to be in good agreement with the Shah and Gilbody [11] experimental measurements, and consistent with the Barna *et al* [7] calculations and the Knudsen *et al* [10] experimental measurements.

To achieve the agreement between theory and experiment found in figure 1 for the single ionization cross sections, we needed to propagate the time-dependent target wavefunction from a time when the projectile was at a distance $d_0 = -50.0$, through closest approach, to a time when the projectile was at a distance $d_0 = +150.0$, which exceeds the box size of $R = 76.8$. An approximate 5% increase in the cross sections was found in going from close-coupling calculations with $\lambda \leq 2$ to those including the octopole terms. Almost no change in the cross sections was found in going from calculations on a $\Delta r = 0.2$ lattice to those on a $\Delta r = 0.1$

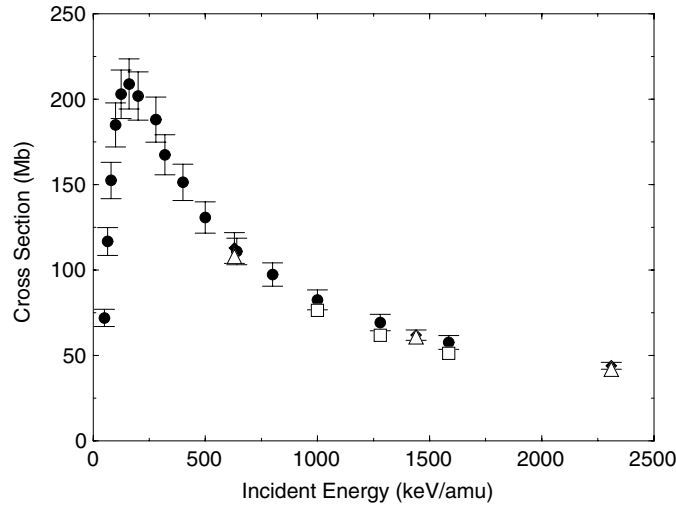


Figure 1. Cross section for single ionization in $\alpha + \text{He}$ collisions. Opaque squares: time-dependent close-coupling results, opaque triangles: time-dependent basis-set coupled channels results [7], solid diamonds: experimental results [10], solid circles: experimental results [11] ($1.0 \text{ Mb} = 1.0 \times 10^{-18} \text{ cm}^2$).

Table 1. $l_1 l_2 LM$ coupled channels.

ss 00
pp 00
dd 00
ff 00
sp 11
sp 10
sp 1-1
ps 11
ps 10
ps 1-1
sd 22
sd 21
sd 20
sd 2-1
sd 2-2
ds 22
ds 21
ds 20
ds 2-1
ds 2-2
sf 33
sf 32
sf 31
sf 30
sf 3-1
sf 3-2
sf 3-3
fs 33
fs 32
fs 31
fs 30
fs 3-1
fs 3-2
fs 3-3

lattice, even though the ground-state energy of He decreased to -78.1 eV . Further consistency checks, such as changing from the bound-state projections of equations (18) and (20) to the bound and continuum state projections of equations (19) and (21), as well as changing from an xz to an xy projectile motion scattering plane for the evaluation of the spherical tensors of equation (13), yielded identical cross sections at all impact parameters.

On the other hand, the time-dependent calculations with 34 coupled channels yielded double ionization cross sections for $\alpha + \text{He}$ collisions that are approximately a factor of 2–3 smaller than the absolute experimental measurements [11]. With the addition of the 67 coupled channels found in table 2, time-dependent close-coupling calculations were carried out with 101 channels ($\lambda \leq 3$) at an incident projectile energy of 1.0 MeV amu^{-1} . The additional channels include ($p \rightarrow d$, $p \rightarrow f$, $d \rightarrow f$) promotions for the pp and dd parts of the fully correlated $ss + pp + dd + ff$ ground state. The single and double ionization weighted probabilities as a function of impact parameter for both the 34 and 101 channel calculations are shown in figures 2 and 3. The change in the single ionization weighted probabilities in going

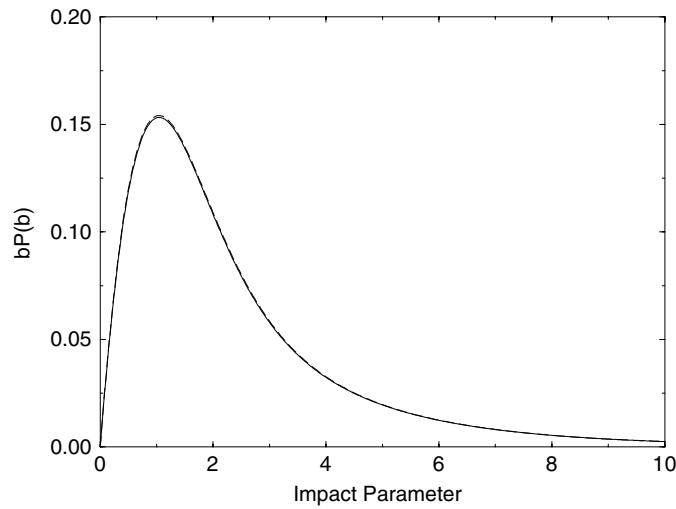


Figure 2. Weighted probability for single ionization in $\alpha + \text{He}$ collisions at an incident energy of 1.0 MeV amu^{-1} . Solid line: 101 channel time-dependent close-coupling results, dashed line: 34 channel time-dependent close-coupling results.

Table 2. Additional $l_1 l_2 LM$ coupled channels.

pp 11	pp 10	pp 1-1				
dd 11	dd 10	dd 1-1				
pd 11	pd 10	pd 1-1				
dp 11	dp 10	dp 1-1				
pp 22	pp 21	pp 20	pp 2-1	pp 2-2		
dd 22	dd 21	dd 20	dd 2-1	dd 2-2		
pd 22	pd 21	pd 20	pd 2-1	pd 2-2		
dp 22	dp 21	dp 20	dp 2-1	dp 2-2		
pf 33	pf 32	pf 31	pf 30	pf 3-1	pf 3-2	pf 3-3
fp 33	fp 32	fp 31	fp 30	fp 3-1	fp 3-2	fp 3-3
dd 33	dd 32	dd 31	dd 30	dd 3-1	dd 3-2	dd 3-3
pd 33	pd 32	pd 31	pd 30	pd 3-1	pd 3-2	pd 3-3
dp 33	dp 32	dp 31	dp 30	dp 3-1	dp 3-2	dp 3-3

from 34 to 101 channels is extremely small, while the change in the double ionization weighted probability is quite large. We note that while the single ionization weighted probability peaks at an impact parameter of approximately 1.0, the double ionization weighted probability peaks at a much smaller impact parameter of approximately 0.4. This decrease in the impact parameter for the peak of the weighted probability in going from single to double ionization is in keeping with that observed in basis-set coupled channels calculations for $\text{O}^{8+} + \text{He}$ collisions [7].

Further time-dependent close-coupling calculations were carried out with 101 channels ($\lambda \leq 3$) at incident projectile energies of 1.280 and 1.585 MeV amu^{-1} . The new 101 channel single ionization cross sections are almost identical to the 34 channel results shown in figure 1. The new 101 channel double ionization cross sections are compared with basis-set coupled channels calculations [7] and absolute experimental measurements [10, 11] in figure 4. The time-dependent close-coupling results for double ionization are found to be in

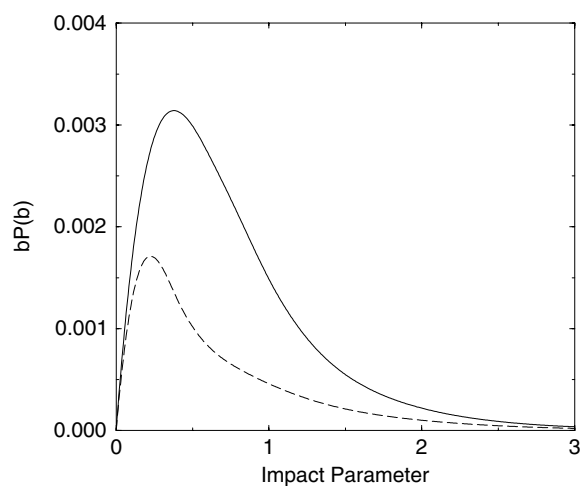


Figure 3. Weighted probability for double ionization in $\alpha + \text{He}$ collisions at an incident energy of 1.0 MeV amu^{-1} . Solid line: 101 channel time-dependent close-coupling results, dashed line: 34 channel time-dependent close-coupling results.

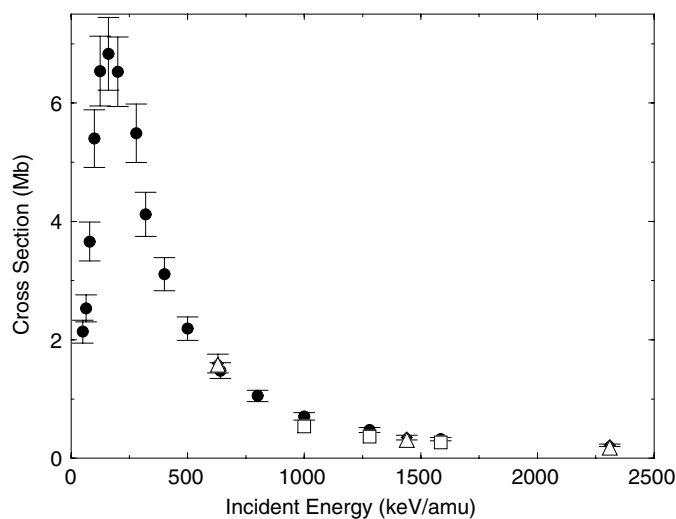


Figure 4. Cross section for double ionization in $\alpha + \text{He}$ collisions. Opaque squares: time-dependent close-coupling results, opaque triangles: time-dependent basis-set coupled channels results [7], solid diamonds: experimental results [10], solid circles: experimental results [11] ($1.0 \text{ Mb} = 1.0 \times 10^{-18} \text{ cm}^2$).

good agreement with the Shah and Gilbody [11] experimental measurements, and consistent with the Barna *et al* [7] calculations and the Knudsen *et al* [10] experimental measurements.

4. Summary

A non-perturbative theory has been developed to treat double ionization processes in fast bare ion collisions with helium. In the approximation that charge transfer processes are small, the resulting time-dependent close-coupling method is based on a target centred two-electron

wavefunction subject to a time-dependent projectile interaction. The time-dependent close-coupling method is then applied to $\alpha + \text{He}$ collisions at incident energies greater than or equal to 1.0 MeV amu^{-1} . In contrast to $\gamma + \text{He}$ collision calculations [2], the $\alpha + \text{He}$ collision calculations are found to be computationally more demanding due to an increase in the number of coupled channels and the need for an extensive range of impact parameters at each incident energy. In the end, absolute cross sections for single and double ionization are found to be in good agreement with recent basis-set coupled channels calculations [7] and absolute experimental measurements [10, 11].

In the future, we plan to apply the time-dependent close-coupling method to calculate ionization processes in other fast bare ion collisions with helium. The extension of the time-dependent close-coupling theory to handle energy and angle differential cross sections for double ionization of helium in collisions with fast bare ions should follow that found before for photoionization processes [13]. In the past, we have found that certain outgoing energies and angles found in the differential cross sections will require many more partial waves and much larger radial meshes than those needed to converge total cross sections. Hopefully, comparisons may then be made with recent experimental measurements [14, 15].

Acknowledgments

This work was supported in part by grants from the US Department of Energy. Computational work was carried out at the National Energy Research Scientific Computing Center in Oakland, California and at the National Center for Computational Sciences in Oak Ridge, Tennessee.

References

- [1] Kheifets A S and Bray I 1996 *Phys. Rev. A* **54** R995
- [2] Pindzola M S and Robicheaux F 1998 *Phys. Rev. A* **57** 318
- [3] Malegat L, Selles P and Kazansky A 1999 *Phys. Rev. A* **60** 3667
- [4] van der Hart H W and Feng L 2001 *J. Phys. B: At. Mol. Opt. Phys.* **34** L601
- [5] McCurdy C W, Horner D A, Rescigno T N and Martin F 2004 *Phys. Rev. A* **69** 032707
- [6] Barna I F, Grun N and Scheid W 2003 *Eur. Phys. J. D* **25** 239
- [7] Barna I F, Tokesi K and Burgdorfer J 2005 *J. Phys. B: At. Mol. Opt. Phys.* **38** 1001
- [8] Deb N C and Crothers D S F 1990 *J. Phys. B: At. Mol. Opt. Phys.* **23** L799
- [9] Bradley J, Lee R J S, McCartney M and Crothers D S F 2004 *J. Phys. B: At. Mol. Opt. Phys.* **37** 3723
- [10] Knudsen H, Andersen L H, Hvelplund P, Astner G, Cederquist H, Danared H, Liljeby L and Rensfelt K G 1984 *J. Phys. B: At. Mol. Phys.* **17** 3545
- [11] Shah M B and Gilbody H B 1985 *J. Phys. B: At. Mol. Phys.* **18** 899
- [12] Pindzola M S and Robicheaux F 1998 *J. Phys. B: At. Mol. Opt. Phys.* **31** L823
- [13] Colgan J and Pindzola M S 2002 *Phys. Rev. Lett.* **88** 173002
- [14] Schulz M, Moshhammer R, Schmitt W, Kollmus H, Feuerstein B, Mann R, Hagmann S and Ullrich J 2000 *Phys. Rev. Lett.* **84** 863
- [15] Fischer D *et al* 2003 *Phys. Rev. Lett.* **90** 243201